EURONOISE 2006
30 May - 1 June 2006 Tampere, Finland

OUTDOOR SOUND PROPAGATION: COMPARISONS BETWEEN CALCULATIONS PERFORMED WITH ATMOS, A PE-BASED MODEL, AND WIND TUNNEL EXPERIMENTS

ABALLEA François, DEFRANCE Jérôme, BAULAC Marine

CSTB
24, rue Joseph Fourier, 38400 Saint Martin d'Hères, France
f.aballea@cstb.fr, j.defrance@cstb.fr, marine.baulac@cstb.fr

ABSTRACT

Noise impact of road and railway infrastructures are more and more severely regulated by national laws: acceptable thresholds and reception levels are decreasing. It becomes necessary to predict more and more finely meteorology and its interactions with boundaries effects in current sound prediction models. ATMOS (Advanced Theoretical Models for Outdoor Sound propagation), a PE (Parabolic Equation) based calculation code dedicated to complex outdoor situations, has been developed to fulfil this need. In order to validate it, a measurement campaign has been performed in the wind tunnel of CSTB, Nantes (France). Such measurements present many advantages compared to outdoor experimentations. The main one is the possibility to control precisely many parameters such as temperature, wind speed profile and wind direction. Aerodynamic measurements as well as computational fluid dynamic simulations with FLUENT have also been undertaken in parallel to acoustical studies. Their results have been used to perform excess attenuation calculations with ATMOS. Comparisons between measurements and numerical simulations for realistic complex traffic noise configurations are presented here for a few cases (flat ground, impedance jump, noise barrier, embankment).

1 INTRODUCTION

ATMOS (Advanced Theoretical Models for Outdoor Sound propagation) is a PE-based (Parabolic Equation) computational code dedicated to complex outdoor situations conjointly developed by CSTB and CEA [1, 2, 3]. A measurement campaign has been performed to compare experimental results with ATMOS results including aerodynamical profiles. This campaign has been carried out on scale models in the wind tunnel of Centre Scientifique et Technique du Bâtiment (CSTB), Nantes (France).The choice of such equipment was made in order to control more easily and more precisely parameters interfering with measurements.

Three typical road traffic configurations are investigated in this paper: a flat ground with a reflective ground, a noise barrier with an impedance jump, and an embankment with an impedance jump.

2 MEASUREMENTS

2.1 Wind Tunnel

The wind tunnel works in closed circuit which gives the ability to control precisely the physical characteristics of the airflow (Fig. 1). The large size of the test room allows a simulation of natural wind speeds from 0 to $30\,ms^{-1}$ ($\pm 0.1\,ms^{-1}$). Different types of roughness can be positioned on the floor at the entrance of the main stream of the tunnel to create different wind profiles and flow turbulences, replicates of real wind profiles between scales $1/20^{th}$ and $1/1000^{th}$.

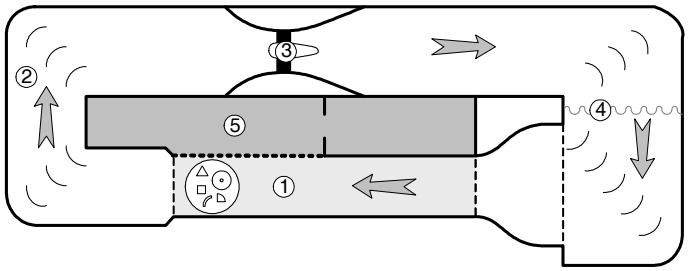

(1) Main stream: length = 20 m, width = 4 m, height adjustable from 2 to 3 m, flow velocity = 0-30 m/s, reduced scale reproduction of natural wind conditions
(2) Return flow
(3) Variable pitch screw propeller
(4) Hot and cold exchanger (temperature control)
(5) Measurement chamber

Fig. 1: Details of the measurement wind tunnel in Nantes

A logarithmic wind speed profile $v(z)$ has been generated at the entrace of the main stream. It is given by:

$$v(z) = a \ln\left(1 + \frac{z}{z_0}\right) \qquad (1)$$

with the refraction parameter $a = 1.12\,ms^{-1}$ and the rugosity length $z_0 = 2.91\times10^{-5}\,m$.

2.2 Acoustic measurements

The sine sweep measurements method [4, 5] is used to get the impulse response of the tested configuration. The frequency response is calculated by FFT after an adapted filter of the

impulse response to delete the unwanted reflections from the ceiling and walls (Fig. 2). A scale of $1/20^{th}$ has been chosen for the experiments so that acoustic measurements have been performed in the frequency range $1000-20000\,Hz$ which corresponds to measurements between $50-1000\,Hz$ at full scale.

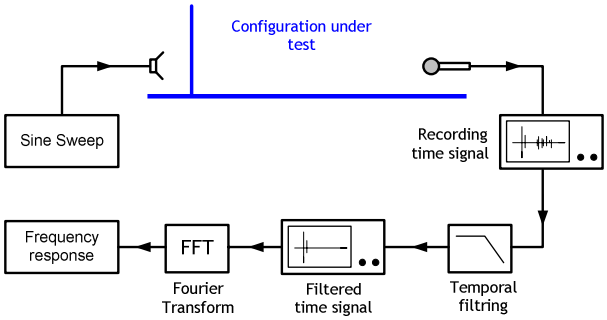

Fig. 2: Measurement principle

3 CALCULATIONS

3.1 ATMOS

The PE-based ATMOS code uses the Helmholtz equation in cylindrical (*r,z*) coordinates for the sound pressure $P(r,z)=\frac{1}{\sqrt{r}}u(r,z)e^{jk_r r}$ with is given by:

$$\left(\frac{\partial^2}{\partial r^2}+\frac{1}{r}\frac{\partial}{\partial r}+\frac{\partial^2}{\partial z^2}+k(r,z)^2\right)P(r,z)=0 \qquad (2)$$

An initial field is propagated step by step from the source to the receiver. After many developments described in Gilbert's article [6], the field at $u(r+\Delta r,z)$ is solved by:

$$\begin{aligned} u(r+\Delta r,z)=\Bigg[&\frac{1}{2\pi}\int_{-\infty}^{+\infty}(U(r,k')+R(k')U(r-k'))\times e^{j\Delta r\left(\sqrt{k_r^2-k'^2}-k_r\right)}e^{jk'z}dk' \\ &+2j\beta\times U(r,\beta)\times e^{j\Delta r\left(\sqrt{k_r^2-\beta^2}-k_r\right)}e^{-j\beta z}\Bigg]\times e^{j\frac{\Delta r\delta k^2(z)}{2k_r}} \end{aligned} \qquad (3)$$

with $U(r,k)=\int_0^{+\infty}e^{-jkz'}u(r,z')dz'$ and $\beta=\frac{k_r}{Z_g}$ with Z_g the normalized ground impedance.

3.2 FLUENT

Wind flow evolution along the sound propagation and in the neighbourhood of the noise barrier or the embankment is computed with FLUENT, a CFD numerical code. The wind speed vectors calculated with FLUENT are taken into account in the numerical code ATMOS as input data via the effective sound speed profile $c(z)$ is given by:

$$c(z)=c_0+\vec{v}.\vec{r}=c_0+v(z) \qquad (4)$$

where $c_0=340\,ms^{-1}$ is the reference sound speed profile, $\vec{v}$ the wind vector and $\vec{r}$ the horizontal direction of propagation.

4 RESULTS

For each of the three studied configuration, the presence of weak wind fluctuations has been observed on measurements results, so that 50 measurements have been done and averaged to get a representative excess attenuation. For numerical calculation, wind speed is supposed to be non turbulent.

4.1 Reflective flat ground

Sound propagation over a reflective flat ground is studied. Configuration and results are presented in Fig. 3. Due to the absence of obstacle, meteorological data calculated by FLUENT are constant along the propagation. For all the receivers, experimental and numerical results show a good agreement, especially concerning the main interference. For the furtherer receivers, the agreement is worst at low frequencies due to a strong background noise of the propeller.

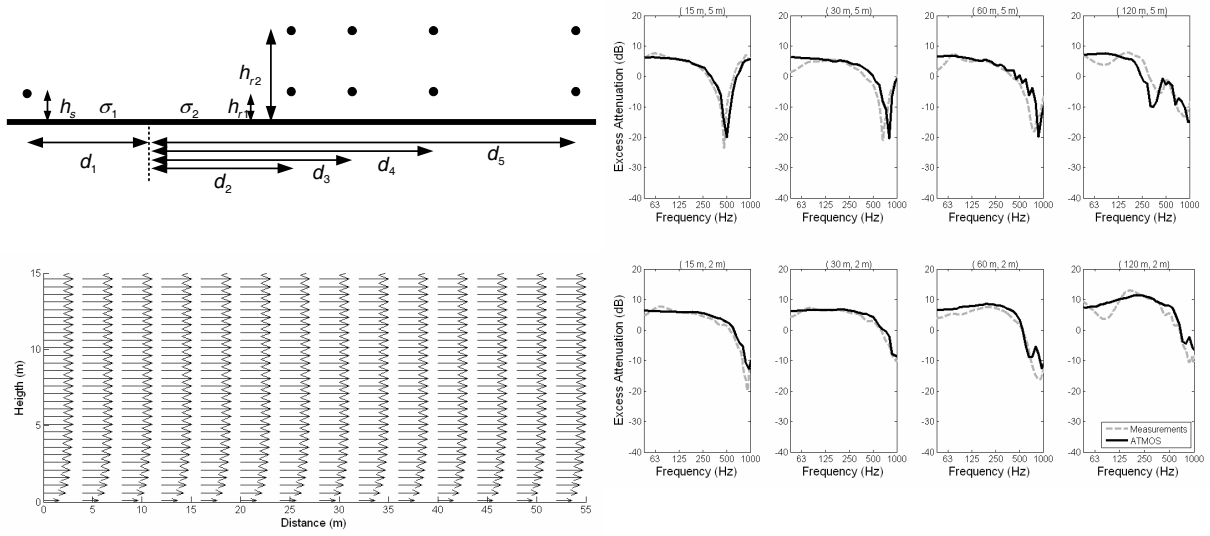

Fig. 3: Flat ground configuration (top-left), FLUENT results (bottom-left), Scale measurements and ATMOS results (right). $h_s = 0.5m$, $h_{r1} = 2m$, $h_{r2} = 5m$, $d_1 = 10m$, $d_2 = 5m$, $d_3 = 20m$, $d_4 = 50m$, $d_5 = 110m$, $\sigma_1 = \sigma_2 = \infty$.

4.2 Acoustic barrier

The configuration described in Fig. 3 is now studied with a 3 meter high acoustic barrier located at $10m$ from the source. The ground behind the barrier is absorbent (Delany and Bazley's model [7] with an air flow resistivity $\sigma_2 = 180 kPasm^{-2}$). The configuration is first studied with FLUENT. Wind speeds profiles are projected on the main propagation direction before being used by ATMOS. Results are presented in Fig. 4.

Results of measurements and ATMOS simulations fit quite well. Like for the configuration with a flat ground, background noise of the propeller is obvious at low frequencies for the most distant receivers. Interferences amplitudes obtained from measurements are less deep due to the measurement averaging but their locations are well respected.

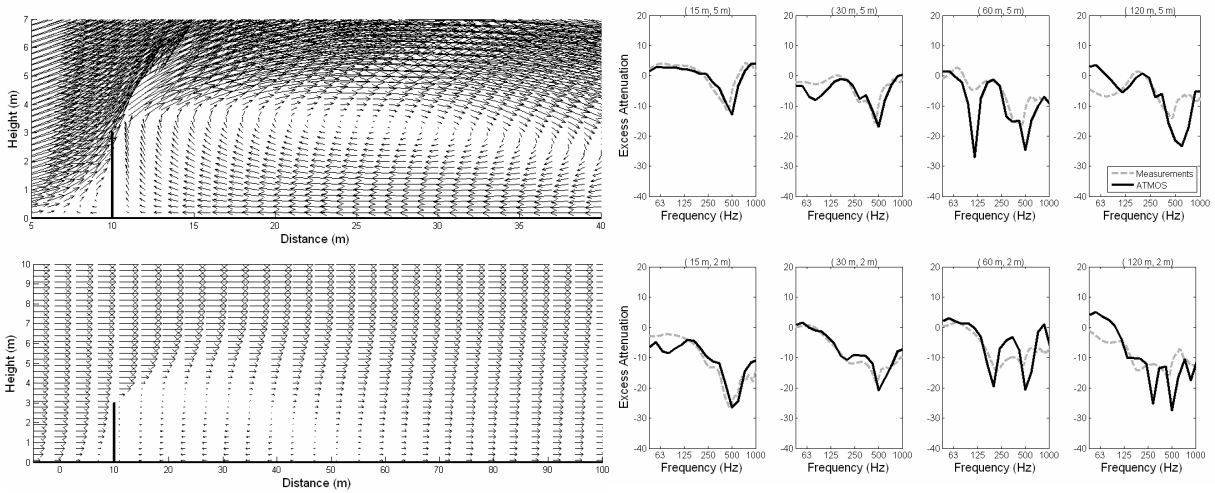

Fig. 4: FLUENT results (upper left) and after being projected on the horizontal direction of propagation (downer left), Scale measurements and ATMOS results (right).

4.3 Embankment

A road embankment is now studied. The configuration is described in Fig. 5. As in section 4.2, the wind speed profiles simulated with FLUENT are projected on the main propagation direction (i.e. parallel to the ground) before being used by ATMOS (Fig. 5). Experimental and numerical results show a good agreement. The propeller background noise perturbation can be observed at closer receivers compared the case in section 4.2.

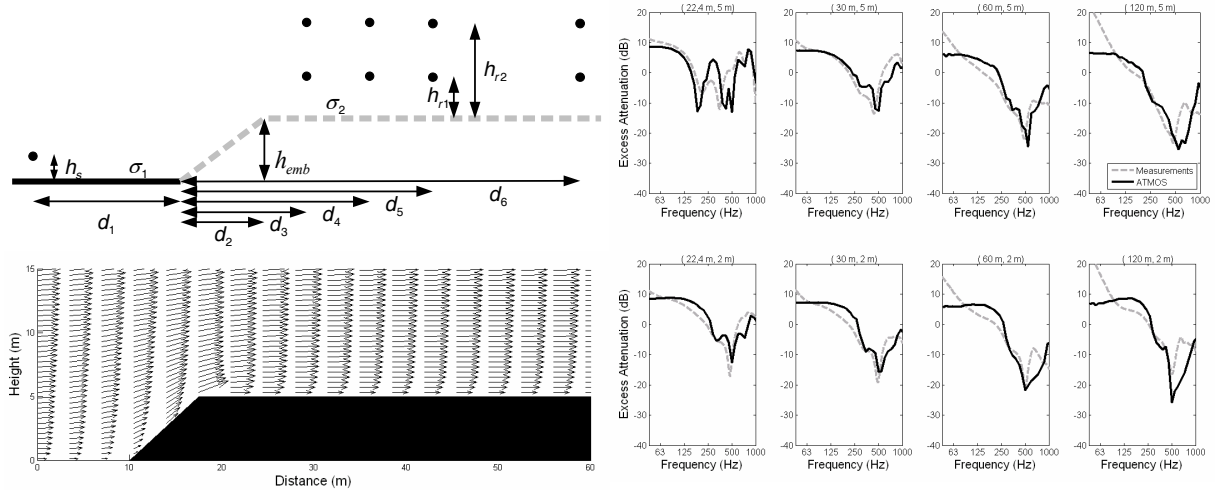

Fig. 5: Embankment configuration (top-left), FLUENT results (bottom-left), Scale measurements and ATMOS results (right). $h_s = 0.5\,m$, $h_{r1} = 2\,m$, $h_{r2} = 5\,m$, $h_{emb} = 5\,m$, $d_1 = 10\,m$, $d_2 = 7.5\,m$, $d_3 = 12.4\,m$, $d_4 = 20\,m$, $d_5 = 50\,m$, $d_6 = 110\,m$, $\sigma_1 = \infty$, $\sigma_2 = 180\,kPasm^{-2}$.

5 CONCLUSIONS

ATMOS can deal with many road traffic noise configurations coupling complex meteorological and topography effects. Even if turbulence effects are neglected in calculations, results show that ATMOS is efficient in the most common complex road traffic noise configurations. Many other cases have been tested during the measurements campaign with different ground geometries and meteorological effects. Work is still in progress to compare these experimental results with new calculations.

REFERENCES

[1] ABALLEA, F. and J. DEFRANCE. Sound propagation over irregular terrain with complex meteorological effects using the parabolic equation model. in Internoise. 2004; Prague, Czech Republic.

[2] ABALLEA, F.-E., Outdoor sound propagation: Application of the fast parabolic equation to meteorological effects and complex topographies (in French). 2004, Thesis, Université du Maine, Le Mans, France.

[3] DEFRANCE, J., F. ABALLEA, M. PRIOUR, E. PREMAT, and P. BLANC-BENON. Sound propagation over non-flat terrain with realistic meteorological effects using the Parabolic Equation: New theoretical developments and comparisons with wind tunnel experiments. in 11th International Symposium on Long Range Sound Propagation. 2004; Fairlee, VT, USA.

[4] FARINA, A. Simultaneous measurement of impulse response and distortion with a swept-sine technique. in AES 108th convention. 2000; Paris, France.

[5] STAN, G.-B., J.-J. EMBRECHTS, and D. ARCHAMBEAU, Comparison of different impulse response measurement techniques. J. Audio Eng. Soc., 2001; **50**(4): 249-263.

[6] GILBERT, K.E. and M.J. WHITE, Application of the parabolic equation to sound propagation in refracting atmosphere. J. Acoust. Soc. Am, 1989; **85**(2): 630-637.

[7] DELANY, M.E. and E.N. BAZLEY, Acoustical properties of fibrous absorbent materials. Applied acoustics, 1970; **3**: 105-116.